

Design for X-Ray Imaging Spectroscopy in Large Helical Device^{*)}

Sadatsugu MUTO and LHD Experimental Group

National Institute for Fusion Science, 322-6 Oroshi-cho, Toki, Gifu 509-5292, Japan

(Received 22 November 2012 / Accepted 27 June 2013)

An assembly of pin-hole camera has been designed for x-ray imaging spectroscopy in Large Helical Device (LHD). In the design the camera basically consists of a 2-D-pixel-array detector, a metallic filter, and a pin hole. The detector measures gray scale images through the filter, while the thickness of the filter changes shot by shot. The gray scale images are mathematically transformed to a color spectral image by means of Mellin transform. The available spectral range is depending on the material of the filter. The spectral energy resolution is also depending on the material of the filter and the intensity of incident x-ray. In the case of the filter made of aluminum, the spectral range is theoretically predicted to be from 3.0 keV to 30 keV. It is also theoretically expected in the case of typical LHD plasmas that 50 frames of color spectral 32×32 -pixel-image is obtained per second with a spectral resolution of $E/\Delta E = 4.3$ at a photon energy of $E = 5.0$ keV.

© 2013 The Japan Society of Plasma Science and Nuclear Fusion Research

Keywords: x-ray, imaging, absorption coefficient

DOI: 10.1585/pfr.8.2402140

1. Introduction

The x-ray spectroscopy for plasma physics is important to study the behaviors of electrons and impurities such as argon and transition metals [1, 2]. Recently, the local emissivities of impurity line and the bremsstrahlung emitted from electrons have been estimated from the time-resolved profiles of x-ray spectra [3]. Especially, it is confirmed that the energy and spatial distributions of the electrons is non-thermal in ECH plasma [4]. In the case of argon impurity, the radial profiles of diffusion coefficient and convective velocity have been estimated [5].

Even in recent advanced technology, the detection principles for the x-ray are basically conventional such as electron excitations in semi-conductors, super-conductors, diffractions from gratings, or refractions from single crystals. Then, in plasma spectroscopy there exists seldom detector which simultaneously satisfies the specific features such as high counting rate larger than the x-ray emissivity, spatial resolution, time resolution, and energy resolution.

In the present research a transformation technique from gray scale images to color spectral image has been invented as an imaging spectroscopy in order to obtain the radial profiles of impurity transports, and the spatial and energy distributions of the electrons in Large Helical Device (LHD). In the technique the x-ray absorptions by material are taken into advantage. Then, the technique is quite different from the conventional ones. In comparison with a pulse-height analyzer for x-ray spectroscopy, it is theoretically expected to obtain the color image with infinite counting rate and no cooling system.

author's e-mail: mutos@ms.nifs.ac.jp

^{*)} This article is based on the presentation at the 22nd International Toki Conference (ITC22).

2. Mellin Transform for X-Ray Imaging Spectroscopy

Photo-absorption effect is applied to the present spectroscopic technique. Especially, it is important that the absorption coefficients in the x-ray region monotonically decrease as the x-ray energy increases except for absorption edges. This fact makes it possible that an incident x-ray spectrum is uniquely obtained from the absorption coefficient and transmission intensity. The mathematical relation between the transmission intensity through an x-ray filter and the incident spectrum is expressed as an integral equation as follows,

$$I(t) = \int_0^{\infty} dE I_0(E) f(E) e^{-\alpha(E)t}, \quad (1)$$

where E , t , $I_0(E)$, $I(t)$, $\alpha(E)$, and $f(E)$ are photon energy, the thickness of the filter along optical axis, the intensity of the incident spectrum, the transmission intensity, the absorption coefficient of the filter, and detection efficiency, respectively. The incident spectrum is the solution of Eq. (1) as follows,

$$I_0(E) = -\frac{1}{2\pi i f(E)} \int_{c-i\infty}^{c+i\infty} ds \frac{g(s)}{G(E, s)}, \quad (2)$$

$$\therefore g(s) \equiv \int_0^{\infty} dt I(t) t^{s-1}, \quad (3)$$

$$\therefore G^{-1}(E, s) \equiv \alpha^s(E) \Gamma^{-1}(s) \frac{d}{dE} \ln \alpha(E), \quad (4)$$

where c , i and Γ are a positive constant, an imaginary unit and a gamma function, respectively. Eq. (3) is a Mellin

transform of the transmission intensity. Then, it is intrinsically necessary for the present spectroscopic technique that the thickness of the filter must be changed shot by shot.

Generally, the absorption coefficient is also depending on the polarization of the incident photon. In the case of magnetized transition metals or rare earth metals, the polarization dependences of the absorption coefficients have been precisely obtained by means of polarized synchrotron radiations in x-ray region [6, 7]. Particularly, the kind of polarization dependences is called a magnetic circular dichroism or a linear dichroism. The dichroisms are given rise to in the vicinity of the absorption edges. In the case of gadolinium the dichroism is close to 100% in the pre-threshold region of 4d-4f excitation [7]. However, the experimentally observed dichroisms are more extended [6, 7]. Those facts are predicted to be due to Fano effect on the quantum interaction between a discrete excitation and continuous excitations. In the case of nickel the extended dichroism is approximately 5% [6]. Significantly, the polarization measurement is available in the region far from absorption edges. The transmission of the polarized spectrum through the magnetized filter is as follows,

$$J_{\pm}(t) = \int_0^{\infty} dE I_{+}(E) f_{+}(E) e^{-\alpha_{\pm}(E)t} + \int_0^{\infty} dE I_{-}(E) f_{-}(E) e^{-\alpha_{\pm}(E)t}, \quad (5)$$

where $I_{\pm}(E)$, $J_{\pm}(t)$, and $f_{\pm}(E)$ are the intensity of incident polarized spectra, the transmission intensity of the polarized spectra, and detection efficiency for the polarized spectra, respectively. The solutions for polarized spectra are as follows,

$$I_{\pm}(E) = -\frac{1}{4\pi i f_{\pm}(E)} \int_{c-i\infty}^{c+i\infty} ds \frac{g_{+}(s) + g_{-}(s)}{G_{+}(E, s) + G_{-}(E, s)} \mp \frac{1}{4\pi i f_{\pm}(E)} \int_{c-i\infty}^{c+i\infty} ds \frac{g_{+}(s) - g_{-}(s)}{G_{+}(E, s) - G_{-}(E, s)}, \quad (6)$$

$$\because g_{\pm}(s) \equiv \int_0^{\infty} dt I_{\pm}(t) t^{s-1}, \quad (7)$$

$$\because G_{\pm}^{-1}(E, s) \equiv \alpha_{\pm}^s(E) \Gamma^{-1}(s) \frac{d}{dE} \ln \alpha_{\pm}(E), \quad (8)$$

Eq. (6) converses to Eq. (2) with no polarization limit.

3. Estimation of Energy Resolution

The energy resolution is estimated from Eq. (2). The infinitesimally narrow spectrum is mathematically expressed by using a delta function as follows,

$$I_0(E) = \delta(E - E_0), \quad (9)$$

where δ and E_0 are the delta function and the energy of the incident photon, respectively. The analyzed result using

Eq. (2) is also the delta function as follows,

$$I_0(E) = \delta(X) \frac{dX}{dE}, \quad (10)$$

$$\because X \equiv \ln \alpha(E) - \ln \alpha(E_0). \quad (11)$$

Then, the ideal energy resolution is proved to be infinite. From Eq. (10) and Eq. (11), the result is also confirmed to be exactly equal to the incident spectrum in the condition that the absorption coefficient monotonically increases or decreases. Consequently, the analysis by using Eq. (2) is restricted to the energy range between the absorption edges. In the case of nickel there are absorption edges at 0.8 keV and 8.0 keV. Then, the energy range for the spectroscopy is between 0.8 keV and 8.0 keV. In the case of copper the range is between 1.0 keV and 9.0 keV.

It is impossible to calculate Eq. (2) exactly by using a computer, since the integration range of Eq. (2) is infinite. Actually, the imaginary part of the parameter of s in Eq. (2), (3), (4) is corresponding to the digit number of parameters in a computational calculation.

In order to avoid the infinite problem, an approximation is taken into account in Eq. (2) as follows,

$$I_{\sigma}(E) = -\frac{1}{2\pi i f(E)} \int_{c-i\infty}^{c+i\infty} ds \frac{g(s)}{G(E, s)} e^{-[\frac{\sigma}{2}(s-c)]^2}, \quad (12)$$

where σ is a parameter meaning the finite integration range. Eq. (12) is equal to Eq. (2) if the parameter of σ is equal to zero. In the same case of the infinitesimally narrow incident spectrum as shown in Eq. (9), the analyzed result is different from Eq. (11) as follows,

$$I_{\sigma}(E) = \frac{1}{\sqrt{\pi}\sigma} \frac{f(E_0)}{f(E)} e^{cX} e^{-\left(\frac{X}{\sigma}\right)^2} \frac{dX}{dE_0}. \quad (13)$$

As is shown in Eq. (13), the parameter of σ is a width of a gaussian and corresponding to the energy resolution. Eq. (13) also converses to Eq. (10) with a zero limitation of the parameter of σ . By means of Talor expansion, the energy resolution at the energy of E is approximately obtained as follows,

$$\Delta E^{-1} \approx \left| \sigma^{-1} \frac{d}{dE} \ln \alpha(E) \right|, \quad (14)$$

where ΔE is defined as the width of the gaussian as same as the parameter of σ .

It is the characteristic feature of the present technique that the energy resolution is depending on the absorption coefficients as shown in Eq. (14). Then, it is available to make the filter from metals or glasses. Particularly, liquids or gases are also possible.

Figure 1 shows the absorption coefficient and the energy resolution of $E/\Delta E$ estimated from Eq. (14) [8]. The absorption coefficient monotonically decreases in the x-ray region above K-edge. However, the energy resolution begins to decrease above the region that the Compton scattering becomes dominant. As a result, the spectral range for the x-ray spectroscopy is from 3.0 keV to 30 keV for the

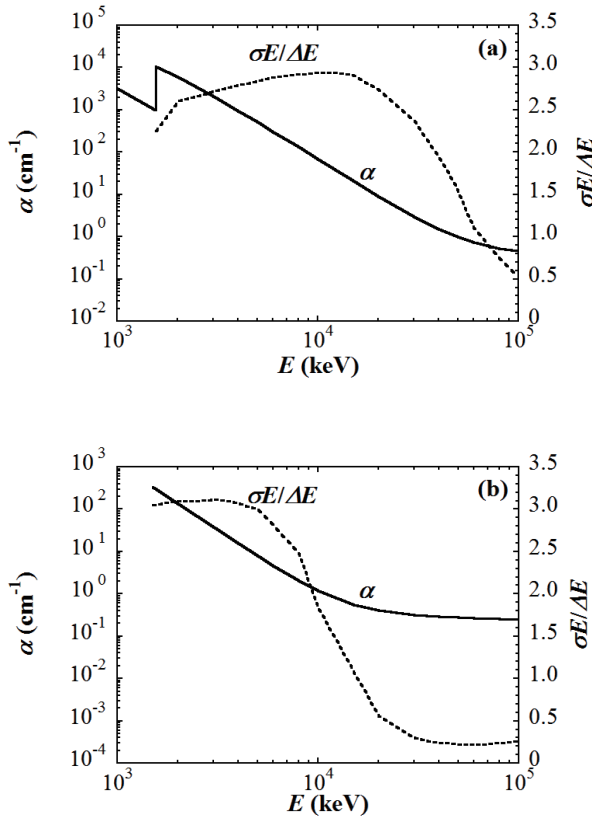


Fig. 1 (a) Absorption coefficient and energy resolution of the aluminum. (b) Absorption coefficient and energy resolution of the beryllium. Solid and broken lines represent the absorption coefficient and the energy resolution calculated from Eq. (14), respectively.

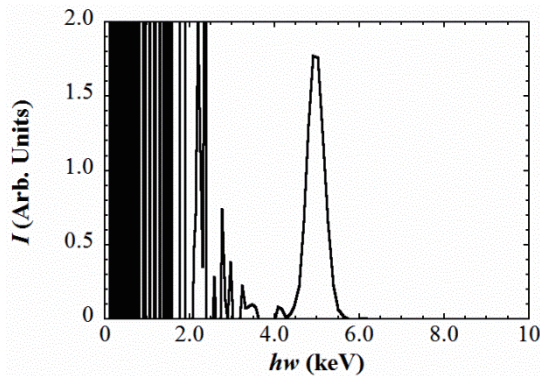


Fig. 2 Calculated result using a personal computer in the case of the aluminum filter. In the analysis it is assumed that the incident spectrum is an infinitesimally narrow line at the energy of 5.0 keV.

aluminum and from 0.8 keV to 8.0 keV for the beryllium, respectively. Above 30 keV, higher Z materials is recommended instead of the aluminum.

Figure 2 shows the numerical analysis obtained with Eq. (12) in an assumption that the incident spectrum is an infinitesimally narrow line. For the analysis a personal computer is used. In the numerical calculation the digit

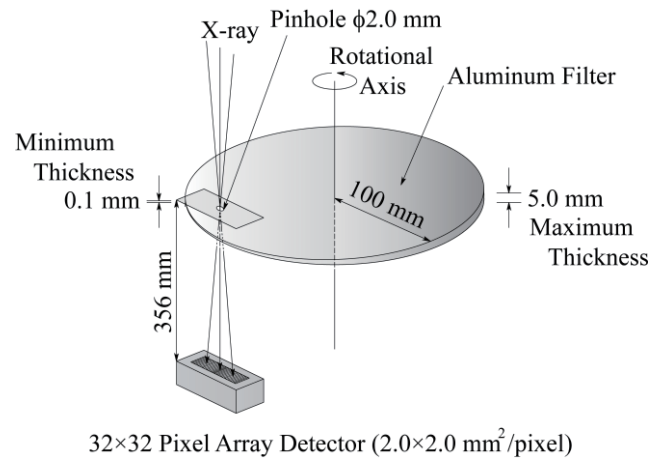


Fig. 3 Geometrical illustration of the assembly. The typical rotation velocity of the filter is 3,000 rpm. The frame rate of the detector is 1 ms. The gray scale images are taken 20 times per rotation. It takes one rotation to obtain a spectral image, if the incident spectrum linearly increases or decreases.

number of parameters is defined to 8. This condition is corresponding to that the incident intensity of $I(t)|_{t=0}$ in Eq. (1) is 16-digits integer as signal intensity, since the relative static error is reciprocally proportional to the square root of the incident intensity. As a result, the actual energy resolution of $E/\Delta E$ is finite and approximately estimated to be equal to 20. This fact indicates that the parameter of σ^{-1} is approximately equal to 6.9, since the energy resolution of $\sigma E/\Delta E$ shown in Fig. 1 (a) is equal to 2.9. Consequently, the parameter of σ^{-1} is equal to the digit number of the signal intensity multiplied by 4.3×10^{-1} .

4. Design of Assembly of Pin-Hole Camera in LHD

The assembly of pin-hole camera has been designed for the x-ray imaging spectroscopy in LHD. The geometrical configuration is illustrated in Fig. 3. The thickness of the filter continuously changes from 0.1 mm to 5.0 mm so that the x-ray above 3 keV can pass through the filter. The time resolution can be controlled by the rotation velocity of the filter. A pin hole is set close to the filter. The assembly is planned to install at a bottom port of LHD. Since the distance between the pin hole and the mid plane of the LHD plasma is approximately 5.0 m, the spatial resolution of 24 mm is to be obtained at the mid plane.

The energy resolution of $E/\Delta E$ is estimated from the x-ray emissivity in LHD. The emissivity integrated between 3.0 and 10 keV is 1.5×10^{18} photons/m³/s in the case of typical NBI plasmas of LHD [3]. This fact means in the case of the configuration that the incident intensity is 2.5×10^6 photons/s/pixel. A single color spectral image is transformed from gray scale images which are measured in a rotation of the filter. Then, the time resolution of the

assembly is 20 ms. The intensity of the incident x-ray is estimated from the flame rate of the detector. In the case of a typical 32×32 -pixel-array detector, the flame rate is 1 ms. Then, the incident intensity is 2.5×10^3 photons/ms/pixel. The parameter of σ^{-1} is approximately expected to be $\log_{10}(2.5 \times 10^3) \times 4.3 \times 10^{-1} = 1.5$. As is shown in Fig.1, the energy resolution of $E/\Delta E$ at 5.0 keV is approximately estimated to be $2.9 \times 1.5 = 4.3$. Accordingly, the energy resolution of the present technique is approximately estimated to be six times less than a semi-conductor detector. On the contrary, the counting rate of the technique is expected to be two orders larger than that of the semi-conductor detector in LHD [9].

5. Summary

An assembly of pin-hole camera is designed to obtain color spectral image in Large Helical Device. The pin-hole camera basically consists of a 2-D-pixel-array detector, a rotational metallic filter, and a pin hole. The detector measures gray scale image, while the thickness of the filter is changed shot by shot. The gray scale images are numerically transferred to color spectral image by means of Mellin transform. The spectral energy range is depending on the material of the filter. In the case of aluminum the energy range is from 3.0 keV to 30 keV. The spectral energy resolution is depending on the absorption coefficient

of the material and the incident intensity of the incident x-ray. By using a typical 32×32 -pixel-array detector, it is theoretically expected in LHD that the energy resolution of $E/\Delta E$ at 5.0 keV is 4.3.

Acknowledgements

The present research is supported by the LHD project budget (NIFS2011ULHH008), KAKENHI (Grant-in-Aid for Scientific Research (C) : 23561001), and the Imaging Science Program of National Institutes of Natural Sciences (NINS).

- [1] K. Ogura *et al.*, J. Phys. Soc. Jpn. **55**, 13 (1986).
- [2] J.E. Rice *et al.*, Phys. Plasma **7**, 1825 (2000).
- [3] S. Muto and S. Morita, Plasma Fusion Res. **3**, S1086 (2008).
- [4] S. Muto *et al.*, Plasma Fusion Res. **5**, S1039 (2010).
- [5] S. Muto and S. Morita, Plasma Fusion Res. **2**, S1069 (2007).
- [6] S. Muto Y. Kagoshima and T. Miyahara, Rev. Sci. Instrum. **63**, 1470 (1992).
- [7] S. Muto *et al.*, J. Phys. Soc. Jpn. **63**, 1179 (1994).
- [8] M.J. Berger *et al.*, XCOM: Photon Cross Section Database (v3.1) [Online] Available: <http://www.nist.gov/physlab/data/xcom> (NIST Gaithersburg, MD, 2009).
- [9] S. Muto *et al.*, Rev. Sci. Instrum. **72**, 1206 (2001).